Rainbow-Link: Beam-Alignment-Free and Grant-Free mmW Multiple Access Using True-Time-Delay Array

Ruifu Li, *Student Member, IEEE*, Han Yan, *Member, IEEE*, and Danijela Cabric, *Fellow, IEEE*

Abstract—The millimeter-wave (mmW) communications is a key enabling technology in 5G to provide ultra-high throughput. Current mmW technologies rely on analog phased arrays to realize beamforming gain and overcome high path loss. However, due to a limited number of simultaneous beams that can be created with analog/hybrid phased antenna arrays, the overheads of beam training and beam scheduling become a bottleneck for emerging networks that need to support a large number of users and low latency applications. This paper introduces rainbow-link, a novel multiple access protocol, that can achieve low latency and massive connectivity by exploiting wide bandwidth at mmW frequencies and novel analog true-time-delay array architecture with frequency dependent beamforming capability. In the proposed design, the network infrastructure is equipped with the true-time-delay array to simultaneously steer different frequency resource blocks towards distinct directions covering the entire cell sector. Users or devices, equipped with a narrowband receiver and either a single antenna or small phased antenna array, connect to the network based on their angular positions by selecting frequency resources within their rainbow beam allocation. Rainbow-link is combined with a contention-based grant-free access to eliminate the explicit beam training and user scheduling. The proposed design and analysis show that rainbow-link grant-free access is a potential candidate for latency-critical use cases within massive connectivity. Our results show that, given less than 10^{-5} probability of packet loss, a rainbow-link cell, over 1 GHz bandwidth using 64 element antenna array, attains sub-millisecond user-plane latency and Mbps user rates with an approximate 400m line-of-sight coverage and a density of up to 5 active single antenna users per second per m^2.

Index Terms—Frequency division multiple access, millimeter wave networks, low latency, critical massive machine type communications, true-time-delay array.

I. Introduction

O NE objective of the 5G evolution is to further diversify its performance and support applications with improved data rates, latency, and number of connected devices. For example, in the emerging Industry 4.0 [1], it is estimated that communications of industrial/intelligent wireless sensor networks (IWSN) in a small cell with up to 1 device per square-meter connection density require 10 to 100 Mbps data rate, with 5 to 30 ms latency, and medium device power consumption and cost [2], [3]. These stringent requirements coincide with all three use categories in 5G specified as enhanced mobile broadband (eMBB), ultra-reliable low-latency communication (URLLC) and massive machine-type communication (mMTC). Specifically, the eMBB is tailored for high peak rate and throughput. General requirements for URLLC are sub 1ms user plane latency and packet error rate as low as 10^{-5} [4]. For mMTC, the general requirement, as suggested by its name, is to provide massive wireless connectivity (e.g. beyond 10^5 links) to machine-type devices in a given area [5].

The millimeter-wave (mmW) communications is a key technology in 5G. Due to abundant bandwidth and antenna array beamforming, mmW communications is the enabler of eMBB. It is also envisioned as a promising candidate for the future high-end IWSN [6]. However, the current mmW solutions have many disadvantages in terms of latency, connection density, power and cost for the industry internet of things (IoT) applications. Firstly, mmW systems rely on beamforming to overcome severe propagation loss. To keep reasonable cost and power consumption, current systems utilize phased antenna arrays at both base station (BS) and user equipment (UE) for beamforming. The overhead associated with beam alignment and beam scheduling using analog arrays is a latency bottleneck. Secondly, the analog phased antenna arrays can connect only a limited number of devices based on the number of beams and the number of radio frequency (RF) chains. Each beamformed transmission occupies the entire bandwidth, therefore frequency domain multiple access cannot be supported. As a result, phased antenna array based mmW networks cannot support a high number of connected devices. Lastly, cost and power consumption of wide-band mmW devices are high which presents a major limitation for IoT applications.

Meeting diversified service requirements with reasonable cost and power consumption is inherently hard. Specifically, to tackle URLLC requirement, key 5G NR features such as grant-free multiple access must be employed [7]. In this
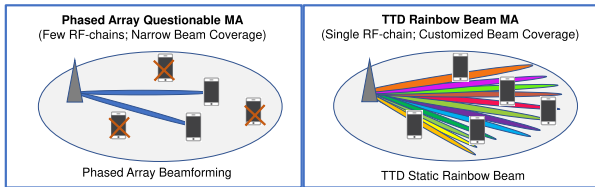
Fig. 1. Due to narrow angular coverage of analog beams, BS with phased array can only serve a limited number of scheduled users. On the other hand, TTD array can connect with users in the entire spatial sector without any scheduling. With phased array, the entire band is pointed to a certain direction, while with TTD array, each beam is pointed to a specific frequency subband (represented by colors).

regime, the network capacity is often limited by insufficient radio resource elements. Reference [8] evaluates URLLC use cases with 10MHz band at 4GHz carrier frequency where the capacity attains 10 users per cell. Alternatively, in mmW band large unlicensed band resources are available. However, due to the need of beamforming, these resources cannot be shared between a large number of spatially separated users [9]. To date, most works that focus on latency in mmW systems emphasize on reducing the initial access and beam alignment latency [10]. Latency due to resource scheduling among multiple users is highlighted by work [11], where optimized frame structure and fully digital arrays were proposed as a solution. The ability of a digital array to connect with users in all directions is useful, however its power consumption and cost is overwhelmingly high. Therefore, to address aforementioned weaknesses of existing solutions for mMTC and URLLC, rethinking of array architectures and multiple access schemes is required.

In this work, we leverage a new beamforming technique referred to as rainbow beam [12], that is enabled by a novel True Time Delay (TTD) array architecture [13]. Rainbow beams exhibit beam patterns that cover the entire angular space by uniquely mapping different frequencies, e.g. orthogonal frequency-division multiplexing (OFDM) subcarrier (SC), onto specific directions. As indicated in Figure 1, rainbow beams are particularly attractive in wideband systems as different SCs and corresponding beamforming directions can be allocated to a large number of users. As long as the users select their appropriate frequency resources, no beam training or scheduling is needed. Based on this feature, in our design a grant free mmW multiple access protocol is combined with rainbow beamforming. It has a potential to provide low user-plane latency for a massive amount of users in IoT applications.

The idea of utilizing frequency dependent beamforming to enhance coverage of directional beams (therefore provide multiple access) has been studied in sub-terahertz communication system [14]–[16]. However, previous studies largely considered broadband, high-rate communications, as opposed to IoT use cases. Differing from most mmW networks, in our design the multiple access based on rainbow beams is regarded as an enabling solution for latency-critical mMTC [17]. On one hand it provides wide angular beam coverage in a power efficient manner by spatially spreading SCs; on the other hand it operates in mmW band where sufficient bandwidth

resources are available to reduce system overhead. Our main contributions are the following:

- We propose a rainbow-beam based frequency domain multiple access which does not require explicit beam-training and supports grant-free random access.
- We propose a detailed design for radio interface, downlink (DL) synchronization procedure, and random access protocol.
- We analyze synchronization performance and probability of collision (packet loss) and their impact on latency for given network design parameters.[1]
- Our analytical study is supported by simulations that evaluate the proposed multiple access scheme in terms of latency, reliability and effective rates.

The rest of the paper is organized as follows. In Section II, we introduce the system model. The proposed rainbow link protocol and radio interface design are included in Section III. The analysis of DL synchronization and uplink (UL) grant-free transmission are presented in Section IV. Section V presents simulation results. Discussion and future work suggestions are in Section VI. The paper is concluded in Section VII.

Notations: Scalars, vectors, and matrices are denoted by non-bold, bold lower-case, and bold upper-case letters, respectively, e.g. h, $\mathbf{h}$ and $\mathbf{H}$. The element in i-th row and j-th column in matrix $\mathbf{H}$ is denoted by $[\mathbf{H}]_{i,j}$. Transpose and Hermitian transpose are denoted by $(.)^{\mathrm{T}}$ and $(.)^{\mathrm{H}}$, respectively. The l_2-norm of a vector $\mathbf{h}$ is denoted by $||\mathbf{h}||$. diag$(\mathbf{A})$ aligns diagonal elements of $\mathbf{A}$ into a vector, and diag$(\mathbf{a})$ aligns vector $\mathbf{a}$ into a diagonal matrix. The i-th element in set $\mathcal{S}$ is denoted as $[\mathcal{S}]_i$.

II. System Model

In this section, we introduce the system model of mmW communication with TTD beamforming. All important notations are summarized in Table I.

We consider a mmW time-division duplex (TDD) network with center frequency f_c and total bandwidth BW. The OFDM waveform with cyclic prefix (CP) is used with a total number of B SCs.

The network consists of a massive number of quasi-static mmW UEs that are served by a BS. We assume each UE, a machine type device, is equipped with a phased array with N_{U} antenna. Furthermore, we assume each UE has much narrower bandwidth than the BS to further reduce power and cost. As a result, each user can only access a subset of SCs through orthogonal frequency-division multiple access (OFDMA). The indices of those SCs accessible by user u are denoted by set $\mathcal{B}_u$ whose cardinality satisfies $|\mathcal{B}_u| \ll B$, i.e., the SCs that a user can access is much smaller than the total number of SCs in the broadband. In practical OFDM based system, adjacent SCs are typically bundled into blocks for frequency resource utilization. This mechanism is controlled by g_{group} which denotes how many SCs are consolidated into a resource block (RB). To be clear on notations, we use $|\mathcal{B}_u|$

---

[1]Our proposed scheme inherently has only two sources of latency due to synchronization and collision with other users that share the same frequency and beam resources.
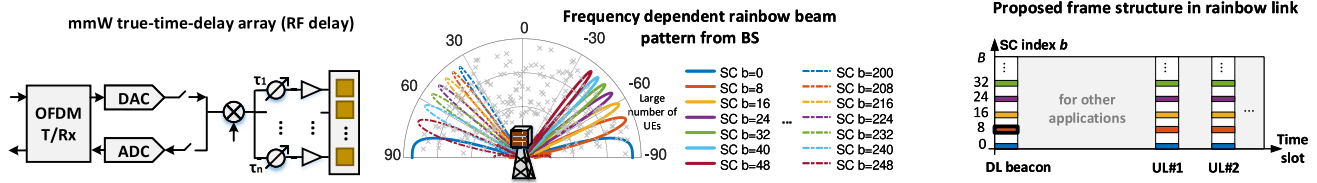
Fig. 2. The left figure shows a typical true-time-delay mmW arrays. The middle figure illustrates the rainbow beam pattern of the base station with $N_\mathrm{B} = 64$ antennas. The BS is in origin point of polar plot and gray crosses represent connected user equipment.

TABLE I

NOMENCLATURE

Symbol	Explanations
Symbols related to system model	
b	Index of SC
$\mathbf{w}_b$	beamformer in the BS for b-th SC
u	Index of UE
$\mathbf{v}_u$	freq independent beamformer at the UE
$\mathcal{B}_u$	SC set a narrowband UE can access
$N_\mathrm{B}, N_\mathrm{U}$	Number of antenna in BS and UE
BW	total bandwidth of the network
M	Number of multi-path components
$\mathbf{H}_{u,m}$	m-th narrowband channel for the u-th UE
$\mathbf{a}_\mathrm{B}(\theta_u), \mathbf{a}_\mathrm{U}(\phi_u)$	Spatial responses of BS and UE
$\phi_u, \theta_u, g_u, \tau_u$	Path AoA/AoD/gain/delay of u-th user
Symbols related to multiple access	
n	Number of repetitions over resource blocks
K	Narrowband cardinality of resource blocks
B	Total number of SC
U	Number of active users per frame
p	Rate of user activation per frame
g_group	Number of SCs bundled into a resource block

for the number of SCs and K for the number of RBs in $\mathcal{B}_u$, i.e., $K = |B_u| / g_\mathrm{group}$.

We assume the BS has a linear array with N_B elements. The antennas are critically spaced, i.e., half of wavelength that associates with f_c. In this work we focus on a sparse geometric channel of M multipath components,[2] where the angle of arrival (AoA), angle of departure (AoD), and complex path gain of the u-th UE and m-th multipath component are denoted as $\theta_{u,m}$, $\phi_{u,m}$, and $g_{u,m}$, respectively. $\theta_{u,m}$ and $\phi_{u,m}$ are assumed to be uniform randomly distributed in region $-\pi/2$ to $\pi/2$. The channel $\mathbf{H}_{u,b}$, for u-th user and b-th SC is

$$\mathbf{H}_{u,b} = \frac{1}{\sqrt{N_\mathrm{B} N_U}} \sum_{m=1}^{M} \alpha_{u,b,m} \mathbf{a}_\mathrm{U}(\phi_{u,m}) \mathbf{a}_\mathrm{B}^\mathrm{H}(\theta_{u,m}) \quad (1)$$

where $\alpha_{u,b,m} = g_{u,m} \exp(j2\pi b \tau_{u,m} \mathrm{BW}/B)$ is the SC-wise complex gain, with $g_{u,m}$ and $\tau_{u,m}$ representing the multipath gain and delay with respect to the first antenna element as a reference. We denote $\mathbf{a}_\mathrm{B}(\phi)$ and $\mathbf{a}_\mathrm{U}(\theta)$ as the narrowband[3] array response vectors, i.e., $[\mathbf{a}_\mathrm{U}(\theta)]_n = \exp[j\pi(n-1)\sin(\theta)]$ and $[\mathbf{a}_\mathrm{B}(\phi)]_n = \exp[j\pi(n-1)\sin(\phi)]$. Amplitude of $g_{u,m}$ is characterized by the free space path loss model [18].

[2]For mmW communication, typically $M \leq 4$.
[3]The narrowband array response model holds true when the propagation delay across the array aperture is less than the sampling duration [12]. For typical mmW BS array aperture ≤ 0.32m, the propagation delay across the aperture is up to 1 ns, which is less than 2.5ns, the sampling duration of a 400MHz system.

In general, channel with multiple taps would be frequency selective. However, since all UEs operate over a small portion of broadband bandwidth, we assume the channel is approximately flat. We also assume the BS is equipped with a reconfigurable TTD array with a single RF chain for its transceiver as shown in Figure 2. In our previous work, we have shown that TTD array can realize frequency dependent beams so that each OFDM SC is mapped to a particular beamforming direction [12]. Delay taps in the array are set to be uniformly spaced with inter-element delay spacing of $\Delta\tau$, regardless of whether the delays are introduced in baseband or RF. The *full-range* rainbow beam[4] can be achieved with tap $\Delta\tau = 1/\mathrm{BW}$ such that the equivalent analog combiner for the b-th SC is given by

$$[\mathbf{w}_b]_i = \exp[j2\pi b(i-1)/B]. \quad (2)$$

Inspecting (2), it is clear that beamformer $\mathbf{w}_b$ steers SC b onto a unique directions with respect to the rest of SCs. On the other hand, any steering vector, i.e., $\mathbf{a}_\mathrm{B}(\phi)$ for an arbitrary ϕ, is also synthesized at a certain SC. Hence it is referred to as full coverage rainbow beamforming. For a certain user, we define $b_u^\star$ as the index of SC whose encoded spatial direction is the closest to the AoA θ_u of a certain path. This particular SC is also denoted as *anchor SC*. In other words, the beamforming gain at anchor SC is the highest among all subcarriers.

To better present our proposed network protocol, we briefly introduce the signal model in the DL and UL. In the DL, we denote the transmit OFDM symbol at the b-th SC as $S^{(\mathrm{DL})}[b]$. Given an ideal bandlimited filter at the UE defined by its narrowband $\mathcal{B}_u$, the received frequency domain signal is

$$R_u^{(\mathrm{DL})}[b] = \underbrace{\mathbf{v}_u^\mathrm{H} \mathbf{H}_{u,b} \mathbf{w}_b}_{\beta_{u,b}} S^{(\mathrm{DL})}[b] + z^{(\mathrm{DL})}[b], \text{ for } b \in \mathcal{B}_u. \quad (3)$$

In the above equation, $\mathbf{v}_u$ represents the precoder of the u-th user (which is not frequency dependent) and scalar $\beta_{u,b}$ characterizes the post-beamforming gain of the b-th SC. $z^{(\mathrm{DL})}[b]$ refers to the noise at the b-th SC..

The received signal at the BS in the UL is expressed as

$$R^{(\mathrm{UL})}[b] = \sum_{u=1}^{U} \underbrace{\mathbf{w}_b^\mathrm{H} \mathbf{H}_{u,b}^\mathrm{H} \mathbf{v}_u}_{\beta_{u,b}^*} S_u^{(\mathrm{UL})}[b] + z^{(\mathrm{UL})}[b] \quad (4)$$

[4]It is noted that this rainbow beam operation has strict requirement on the delay range of the circuit blocks that introduce delay. However, with the increased bandwidth in mmW and sub-THz, as well as the recent break-through of circuits [19], such regime is attainable.

where the post-beam channel gain in the UL $\beta^*_{u,b}$ is the conjugate of the one in the DL as long as the same SC and UE-side beamformer $\mathbf{v}_u$ is used.

Since each SC is mapped to a spatial direction, UE can measure the receive power on SCs during DL boardcasting and identify the segment of SCs with the highest received power as the segment aligned with its AoA. Note that although the channel gain is assumed to be flat across the narrowband $\mathcal{B}_u$, post-beamforming gain $\beta_{u,b}$ is still frequency dependent (b dependent) due to TTD beamforming precoder $\mathbf{w}_b$ at the BS side. This unique feature of rainbow-beam with TTD array causes beamforming gain loss on different SCs. Even if a UE has broadband sampling capability, there will only be certain SCs that it can use. This design consideration is addressed in Section IV .

III. RAINBOW LINK MEDIUM ACCESS CONTROL

In a conventional mmW UL access, a 4-step random access procedure is employed. The BS broadcasts synchronization and beam training pilots during DL. The UEs independently conduct synchronization, measure the received signal strength of BS's beams, and send feedback through the random access channel. After the BS receives feedback, it applies user scheduling and resource allocation scheme by reserving dedicated time-frequency resources for UEs before sending them access grant. UEs then use the scheduled resources to complete UL transmission. In this scheme a non-trivial latency is expected not only in the grant request, but also in the resource scheduling because the served UEs in each time slot are limited to a small angular region covered by a narrow analog beam from the BS.

The rainbow link on the other hand, leverages the frequency-dependent beam steering capability of TTD array which can simultaneously connect multiple UEs. We propose to use a fixed beam configuration given by beamforming precoder/combiner in (2) for both DL synchronization and UL access, i.e., on the BS's side no beam switching is required. Due to large coverage of rainbow beam in angular domain, UEs always have beamforming gain to and from BS without explicit beamforming training or feedback. Elimination of beamforming feedback significantly cuts the overhead on beam maintenance and resource scheduling which then makes the 2-step contention based random access possible.

This section presents the proposed protocol for multiple access with rainbow link. We start by discussing details of DL synchronization and UL grant-free transmission. Based on the discussion, we then provide the design of radio interface as well as relevant performance metrics that are analyzed in Sections IV and V.

A. Rainbow Beam DL Synchronization

Given a wideband OFDM transmission from the BS, the synchronization of the narrowband UEs require estimation of the correct timing offset and fast Fourier transform (FFT) window for decoding. Effectively, a narrowband receiver at the UE side needs to select a set of SCs $\mathcal{B}_u$ that are then used for UL transmission. Since rainbow beam maps each

SC to a specific spatial direction, UEs should select SCs that are mapped to its AoD so that they leverage the maximum beamforming gain from BS and improve DL for the detection of the synchronization signal. Due to narrowband receiver processing at the UE, the synchronization involves following challenges:

- UEs should synchronize using a received signal that contains only a fraction of the entire OFDM preamble.
- UEs needs to locate (in the frequency domain) a segment of SCs with the minimum beamforming gain loss as its operating band $\mathcal{B}_u$.

To tackle the first challenge, we propose to load synchronization sequences on all SCs. Since the AoD of a UE in DL channel might land on any SC across the wideband, we employ pseudorandom noise (PN) sequences instead of Zadoff-Chu sequences that are used in 4G Narrowband Internet of Things (NB-IoT). PN sequences have a low peak to average power ratio, zero auto-correlation with its time-shifted version, and do not require fixed narrowband reception for completeness [20]. The preamble sequence is assumed to be known at UEs.

The second challenge is essentially dependent on the UE's ability to maintain beam alignment with the BS. With no prior information about which segment it should select, a UE would have to traverse the entire broadband signal and repeatedly search for $b^\star_u$, the anchor SC with the highest beamforming gain. Undoubtedly, traversing the entire broadband frequencies (with low sampling rate) would cause prohibitive overhead. We assume that UEs are quasi-static and thus the AoDs change slowly. In this case, using the previously selected segment as a prior, UEs can keep track of changes in AoDs. This simplification eliminates the extra overhead of UEs searching for $b^\star_u$.

As illustrated in Figure 2, synchronization sequences are loaded onto different SCs in the DL broadcast. The DL synchronization signal contains frequency multiplexed narrowband beacons.[5] In order to participate in contention UEs are required to successfully synchronize. The synchronization algorithm at the UE involves the following steps:

- Perform down conversion by multiplying the broadband signal with $\exp(-1\mathrm{j}2\pi t b^\star_u/B)$, filtering, and sampling to obtain a narrowband baseband signal. $b^\star_u$ here refers to the anchor SC from the previous connection.
- Locate the correct FFT window by estimating the integer and fractional timing offset.
- Identify the new anchor SC $b^\star_u$ with the highest signal strength. The updated $\mathcal{B}_u$ for UL transmission is determined accordingly.

B. Rainbow Beam UL Grant-Free Transmission

The proposed work cycles and the corresponding timing diagram of the UL grant-free protocol is shown in Figure 3. When their packets are generated, each UE activates and

---

[5]This concept is similar to NB-IoT where a narrowband synchronization sequence is loaded in resource block. What is unique in rainbow link is that each anchor carrier is coded with a unique analog beam.

(a) BS & UE Work Cycles
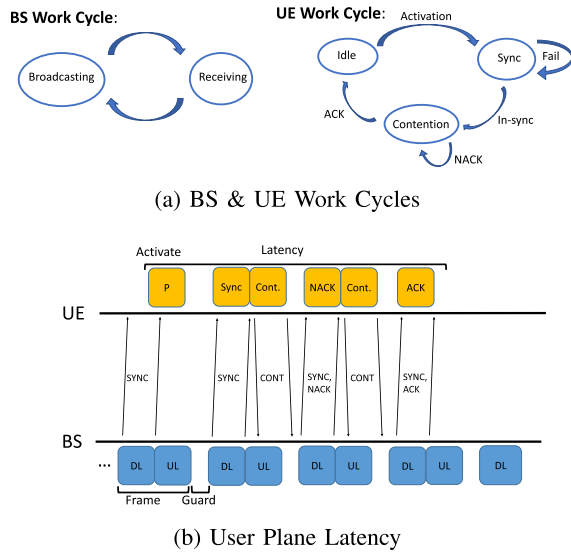

(b) User Plane Latency

Fig. 3. The uplink grant-free access with proactive repetition scheme similar to [22] and [23]. The abbreviation **P**, **Cont**, **ACK**, and **Sync** denote packet arrival, contention attempts, ACK and synchronization attempts, respectively. A short guard period counts for propagation and processing delay. In the diagram, UE succeeded in the first synchronization attempt and the second contention attempt.

synchronizes in the nearest DL time frame where BS broadcasts synchronization signal, after which UE transmits in an arrive-and-go manner. Namely, UE does not send a scheduling request for access grant as in grant-based access. For the UL transmission it utilizes multiple RBs in the narrow band centered[6] at the detected anchor SC, i.e., $\mathcal{B}_u = [b_u^\star - |\mathcal{B}_u|/2, b_u^\star + |\mathcal{B}_u|/2-1]$. UEs are sending packets that contain preamble and data so that BS can extract UE's identity and other necessary control information.

Naturally in a grant-free access, multiple packets transmitted in the same time-frequency resource block from different UEs would cause a collision and packet loss. For the sake of tractable analysis, we assume decoding on SCs without collision always succeeds, and decoding on SCs with collision always fails. In order to improve the packet loss rate, we propose a simple repetition coding. With abundant time-frequency resource blocks in mmW spectrum, UEs can perform repetitive transmissions on multiple resource blocks [21]. In our proposed scheme, each UE repeats its transmission on n RBs in its narrow band of K RBs. The n replicas offer repetition coding and diversity gain to reduce packet loss. Making a large number of repetitions alleviates the loss of packets for a certain user. But the contention also becomes harsh when other UEs do so. In this work we assume a fixed number of repetition n for all users and study the optimal design of n. Notice that the optimal n will also be influenced by the notion of grouping. When multiple SCs are consolidated as a RB, UEs load more useful symbols into a packet but have less resources to avoid collisions. We will analyze these trade offs in Section IV.

TABLE II

NUMEROLOGY

Specification	Value
Sampling Frequency[MHz]	983.04
Number of Points in FFT	2048
BW [MHz]	1000
SC Spacing [kHz]	480
Cyclic Prefix [Samples]	256
Symbols per TTI	13
Symbol Duration [μs]	2.083
Symbol Duration with CP [μs]	2.344
TTI Duration [μs]	30.469

C. Radio Interface Design

In order to analyze rates, coverage, and latency of the proposed system, this section briefly discusses radio interface design. Due to its popularity, reliability, and flexibility for contention based grant-free random access [23], we adopt a frame slotted Aloha. Both UL and DL transmissions are slotted in terms of frames[7] and users can transmit without grant request or allocated resources from BS. Critical specifications in radio interface for the proposed system include [25]:

- Subcarrier spacing and OFDM symbol duration.
- Cyclic prefix to accommodate combined channel delay spread and the largest delay tap of TTD array
- Number of UL & DL TTIs
- Length of UL & DL preamble
- Payload in DL frames

In URLLC and mMTC use cases, short packets are commonly used [26], [27]. In that sense, large spacing between SCs shall be considered. A natural choice is then to adopt a numerology scaled from the current 5G and 4G networks. As pointed out by [28], in current standards, SC separation (SCS) is of the form: $2^k \times 15$kHz for integer k. Specifications with $k > 2$ cannot be implemented in sub-6GHz spectrum. To get a rough understanding of the system, we then use the $k = 5$ case as listed in Table II. Here the length of CP is about 250ns which is sufficient to accommodate the combination of largest delay of TTD element[8] and the root mean square delay spread of mmW frequencies in most outdoor environment [18].

Each frame would contain multiple transmission time interval (TTI)s. Frame length is a critical design to accommodate various control data and payloads. With the grant-free multiple access, the structure of DL TTI in the proposed scheme is relatively simple. The detailed frame structure is specified in Table III.

Although BS transmits wideband signals, only a portion of the band is accessible to each narrowband UE. Therefore both UL and DL reference signals (preambles) in our design are much longer than the ones in [25] due to lack of broadband receiving capabilities. We also assume open-loop power control with a maximum UE transmit power of 23 dBm [29]

---

[6]From a geometric argument, putting the anchor SC in the center of $\mathcal{B}_u$ intuitively ensures that there is good channel gain.

[7]The propose protocol utilizes subset of time-frequency resource, similar to the interleaved NB-IoT resource units with LTE [24], and we focus on relevant UL/DL only.

[8]The largest delay is N_B samples as specified by size of the array. 256 samples could accommodate a 128 element array.

TABLE III

FRAME DESIGN

| Specification	Design Values
UL Symbols [TTI]	2
DL Symbols [TTI]	2
Frame Length [μs]	125
Frame Length [symbols]	52
DL Reference Signal [symbol]	22
DL Control Signal [symbol]	2
Guard Interval [symbol]	2
UL Preamble [symbol]	8
UL Payloads [symbol]	18

Fig. 4. The narrowband operation of UE and rainbow beams naturally reject multipath components. For signal at a given subcarrier, its multi-path components propagate via a different AoD and hence are filtered out by UE due to its limited bandwidth.

which allows for shorter UL reference symbols than that of DL frame.

The proposed numerology and frame design are used throughout the rest of the paper. It is worth mentioning that this numerology is tailored to achieve URLLC with large SC spacing and mini-slots. In general, depending on the application, there are designs with more efficient control fields. However, these investigations are beyond the scope of this paper.

D. Performance Metrics

To simplify the discussion, we assume that a successful DL synchronization and UL transmission without collision together lead to a successful packet delivery. During each DL broadcasting, BS encodes feedback per SC to indicate whether previous UL payload on that SC is successfully decoded. Synchronized UEs would persistently transmit until their packets are delivered, while UEs with unsuccessful synchronizations do not participate in contention. The probability of successful synchronization is dependent on the receiver DL preamble. For users that are within the rainbow link coverage, we analyze the following performance metrics:

- Access latency: defined as the amount of time between packet arrival and its successful delivery.
- Effective rate: defined as the ratio of the number of data symbols (payload) in a packet and the time required to successfully delivery through contention.

Both metrics depend on several factors including SNR, user density, the number of repetitions, and grouping of subcarriers into RBs.

The proposed system is expected to serve a large number of spatially separated users with low latency. In the next section, we analyze DL synchronization and UL contention, and mathematically formulate performance metrics.

IV. PERFORMANCE ANALYSIS OF RAINBOW LINK

In this section, we provide analysis of the proposed rainbow link access. For the sake of tractable analysis and concise notation, we make two additional assumptions. Firstly, we mainly focus on a single path channel, i.e., the summation and the m-dependency in (1) are dropped. The underlying rationale is that each UE can only access a narrow bandwidth $\mathcal{B}_u$, therefore it is very likely that only a single path aligns in the spatial direction encoded on SCs within $\mathcal{B}_u$ as illustrated in Figure 4.
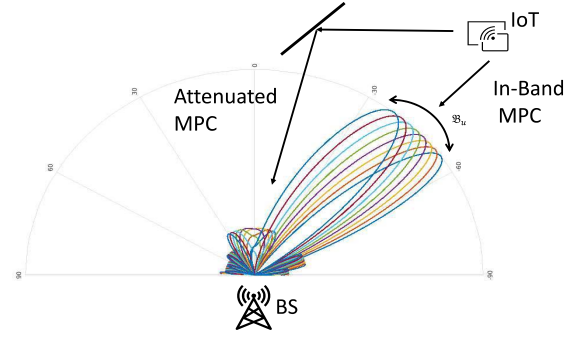
Secondly, we omit the discussion of beamforming in the UE's side. Specifically, $N_{\mathrm{U}} = 1$ is used, and we drop beamformer $\mathbf{v}$ and array response $\mathbf{a}_{\mathrm{U}}(\phi_u)$ of UE in the analysis. The rationale behind is that in the term $\beta_{u,b} = \mathbf{v}_u^{\mathrm{H}} \mathbf{H}_{u,b} \mathbf{w}_b$, UE's beamformer serves merely as another factor that has no dependency on b. In other words, a multi-antenna UE results merely in a higher beamforming gain and is not related to any unique feature of rainbow beamforming.[9]

A. Analysis of DL Synchronization

Synchronization based on OFDM waveform usually involves estimation of timing offset and carrier frequency offset [30]. With TTD array, in addition to timing offset UEs need to locate their anchor SCs. Here we employ a similar analysis as in [30] of NB-IoT without addressing the carrier frequency offset. In order to locate the anchor SC $b_u^\star$ with the highest gain during DL synchronization, a user needs to find:

$$b_u^\star = \mathrm{argmax}_b |\beta_{u,b}|^2 \qquad (5)$$

$b_u^\star$ is then the anchor SC whose steering angle is the most aligned with θ_u. Plugging (1), (2) into (3) and simplifying:

$$|\beta_{u,b}|^2 = \frac{|\alpha_u|^2}{N_{\mathrm{B}} N_{\mathrm{U}}} \underbrace{\left| \frac{\sin \left[\frac{N_{\mathrm{B}} \pi}{2} \left(\frac{2b}{B} - \sin \theta_u \right) \right]}{\sin \left[\frac{\pi}{2} \left(\frac{2b}{B} - \sin \theta_u \right) \right]} \right|^2}_{F_{N_{\mathrm{B}}}(\pi \zeta / B)} \qquad (6)$$

The expression above leads to Fejér kernel $F_{N_{\mathrm{B}}}(\cdot)$ which is defined as $F_N(x) = |\sin(Nx/2)/\sin(x/2)|^2$. $b_u^\star$ should then satisfy the following criterion:

$$-1 \leq 2b_u^\star - B \sin \theta_u \leq 1$$

From (6), one can see that as the total number of SCs in UE's band increases, the edge SC $b_u^\star \pm |\mathcal{B}_u|/2$ have an increasing gain loss compared with the anchor SC $b_u^\star$. This has two implications. Firstly, to ensure a relatively flat beamforming gain across the UE narrowband bandwidth, the

---

[9]Presumably, using multiple antennas on UE side also requires extra overhead for beamforming training.

total number of SCs in the broadband should be much larger than number of antennas at the BS N_B, i.e., $N_B/B \ll 1$. This is because the gain difference in narrow band is only relevant to the ratio N_B/B as shown in (6). Secondly, due to the gain loss, there are only limited number of SCs that can be included in $\mathcal{B}_u$. For instance, a generic threshold $|\mathcal{B}_u| \leq B/N_B$ ensures that the SC at the edge of $\mathcal{B}_u$ has less than 3dB gain loss compared with the anchor SC . Increasing number of antennas N_B at the BS might result in large gain difference which then limits SCs that a user can access. Notice that these phase and gain differences do not affect UL data transmission since they can be treated as part of the channel. With UL preamble sequence, BS estimates the channel per SC and thus naturally compensates it.

The rest of the subsection then addresses the estimation of timing offset. Let L denote the number of symbols in DL preamble sequence. Let l be the index of samples in a OFDM symbol such that $-N_{CP} \leq l \leq |\mathcal{B}_u|$. Then l-th sample of the m-th symbol in preamble sequence can be expressed as:

$$s_u^{(DL)}[l;m] = \sum_{b \in \mathcal{B}_u} g_u \left[\mathbf{a}_B^H (\theta_u) \, \mathbf{w}_b \right] S_u^{(DL)}[b;m] e^{1j2\pi \cdot \frac{b}{|\mathcal{B}_u|}(l-D_u)}$$
$$+ z[l;m] \qquad (7)$$

where D_u amounts to normalized timing offset that includes an integer and a fractional part due to down sampling. In the equation above, only SCs within the narrow band $\mathcal{B}_u$ are taken into account. This assumes that UEs sample the wideband signal without aliasing. In practice, such assumption can be achieved with a high quality low pass filter. With channel gain g_u remaining the same for $\mathcal{B}_u$ during L symbols, the received frequency domain symbol is then:

$$\tilde{S}_u^{(DL)}[b;m] = g_u \left[\mathbf{a}_B^H (\theta_u) \, \mathbf{w}_b \right] S_u^{(DL)}[b;m] e^{1j2\pi \cdot \frac{b}{|\mathcal{B}_u|}(-D_u)}$$
$$+ \tilde{z}[b;m] \qquad (8)$$

In (8), $\tilde{z}$ is the per SC noise in frequency domain. Synchronization is essentially an estimation of D_u from observed samples $\tilde{S}_u^{(DL)}[b;m]$. However, since θ_u is unknown, the gain loss cannot be accurately modeled and causes degradation in synchronization performances. We evaluate the following estimator for timing offset and its synchronization performance:

$$D_u^* = \arg\max_{D_u} \ |J_u(D_u)|^2$$
$$J_u(D_u) = \sum_{m,b} \left(\tilde{S}_u^{(DL)}[b;m] \right)^* S_u^{(DL)}[b;m] \times e^{1j2\pi \cdot \frac{b}{|\mathcal{B}_u|} D_u}$$
$$(9)$$

In (9) UEs merely perform correlation between $\tilde{S}_u^{(DL)}[b;m]$ $S_u^{(DL)}[b;m]$ when estimating D_u^*. As $|\mathcal{B}_u|$ increases, the summation in (9) involves more symbols, but the correlation between the two sequences is also more distorted. To conclude, in DL synchronization UEs suffer from gain loss due to the rainbow beam pattern and can therefore only operate on a limited number of SCs. This effect will be analyzed via numerical simulations.

We note that as a unique feature of frequency dependent rainbow beam pattern, the synchronization does benefit from

beamforming gain contributed by BS antenna. The length of preamble L should be designed accordingly to fulfill high probability of detection and low synchronization error.

B. Analysis of Packet Loss Rate

Next we analyze collisions and packet loss rate (PLR) for given radio resources and user density. The purpose of the analysis is to mathematically guide the design of various system parameters.

Since UEs are narrowband, there is no collision between UEs that contend in non-overlapped bands. Given that all users choose a consecutive K RBs, a subband would suffer from collisions from users landing on a total number of $2(K-1) + 1 = 2K - 1$ RBs. To tackle all the possibilities for a given number of repetitions, a combinatorial approach is needed. In the analysis, we focus on a specific user occupying bandwidth $\mathcal{B}_u$ and calculate the density function of the number of occupied SCs in the band before this user adds its replicas. From there, packet loss rate is simply the probability that all replicas from this user are covered by already occupied SCs. Based on our model, the packet loss rate $P_{PLR}(B, K, U, n, g_{group})$ is given in the following proposition as a function of the number of SCs B, the number of active users U, the number of RBs that a user can access K, the grouping factor g_{group}, and the number of repetitions n for each user.

Proposition 1: With a uniform spatial distribution of users, an approximated expression of PLR of the proposed rainbow link is

$$P_{PLR} = \sum_{i=1}^{U-1} f\left(U-1, g_{group} \frac{2K-1}{B}, i \right) \sum_{j=n}^{K} \left[\mathbf{T}^i \mathbf{p}_0 \right]_j \frac{C_j^n}{C_K^n},$$
$$(10)$$

where $f(x, p, i) = C_x^i (1-p)^{x-i} p^i$ is the binomial probability distribution function, C_x^i is the operator that evaluates x choose i, $\mathbf{p}_0 = [1, 0, \cdots, 0]^T \in \mathbb{R}^{K+1}$ is the unit vector, and the entry in m_1-th row and m_2-th column of the matrix $\mathbf{T} \in \mathbb{R}^{(K+1) \times (K+1)}$ is given by

$$[\mathbf{T}]_{m_1,m_2} = \frac{C_{K-m_1}^{m_2-m_1} C_{m_1}^{n-(m_2-m_1)}}{(2K-1)C_K^n}$$
$$+ \sum_{j=0}^{n} \sum_{k=2}^{K} \frac{2C_{K-k}^{n-j} C_{K-m_1}^{m_2-m_1} C_{m_1}^{j-(m_2-m_1)}}{(2K-1)C_K^n}. \quad (11)$$

Proof: See Appendix A. ∎

We note here that with all other parameters fixed, P_{PLR} as a function of n has a minimum. However, since n is an integer and the formula in (10) is complicated, we discard discussions on conditions of optimal n. In practice, we can simply calculate P_{PLR} numerically for purposes of system design.

In general, increasing the number of SCs that a UE accesses can drastically reduce packet loss rate. However, from a geometric perspective, the generic argument is that $|\mathcal{B}_u|$ is limited by B/N_B, the number of spatial directions in the main lobe of an analog beam. This can also be seen from (8) that SCs outside of the main lobe of $b_u^\star$ have large gain loss.

C. Latency and Rate Calculation

With both major causes of protocol overhead addressed, in this subsection we discuss the performance metrics used in the evaluation of the system. Since the system is designed to fulfill stringent latency requirements, we mainly focus on the overall latency. Based on latency analysis, we then derive the formulas for effective data rate of UEs.

As illustrated by Figure 3, the overall latency T_{tot} can be computed as follows:

$$
\begin{aligned}
T_{\text{tot}} &= T_{\text{sync}} + T_{\text{cont}}, \\
T_{\text{sync}} &= T_{\text{activation}} + T_{\text{failure}} + T_{\text{DL}}, \\
T_{\text{cont}} &= T_{\text{packetloss}} + T_{\text{DL}}.
\end{aligned}
\tag{12}
$$

Specifically, $T_{\text{activation}}$ accounts for the random offset to the nearest broadcasting when a UE activates. T_{failure} accounts for unsuccessful synchronization attempts which might include multiple frames. The extra T_{DL} is the overhead for successful synchronization. In T_{cont}, $T_{\text{packetloss}}$ stands for packet loss in contention and the extra T_{DL} stands for the overhead receiving ACK from DL broadcasting.

The equation to calculate the effective rate is:

$$
R_{\text{eff}} = \frac{N_{\text{payloads}}}{T_{\text{cont}}} = \frac{g_{\text{group}} N_{\text{packet}}}{T_{\text{cont}}}
\tag{13}
$$

where N_{payloads} is the total payload and N_{packet} is the payload per packet in terms of OFDM symbols.

The most non-trivial trade-off in our proposed design is controlled by g_{group}. On one hand, as indicated by the numerator in (13), using a large number of SCs per RB (large g_{group}) boosts the data rate of UEs. On the other hand, large g_{group} also enlarges the denominator in (13) through (12), (10). The interpretation is that given a fixed $|\mathcal{B}_u|$, increasing g_{group} enhances useful payloads but also reduces the number of RBs which means UEs become more vulnerable to collisions.

Since the contention overhead depends on the number of users participating in contention at that time, it is hard to evaluate it analytically. Simulation results will analyze these performance metrics in the next section.

V. NUMERICAL AND SIMULATION RESULTS

In this section, we support our analysis in the previous sections with numerical results. We start with a brief illustration on how certain system parameters are chosen in the simulations.

- *Size of BS antenna* N_B: As discussed in Section IV, N_B limits the size of the set $\mathcal{B}_u$, i.e., SC that the u-th user uses. In simulation, the number of antenna is set to $N_B = 64$. This enables the UEs to access at most $|\mathcal{B}_u| \leq B/N_B = 32$ SCs in its narrow baseband within 3dB gainloss with $B = 2048$ as specified by the number of points in Table II. The UE's baseband bandwidth is then approximately 16MHz.
- *Grouping factor* g_{group}: To keep the discussion simple, we assume that for each user, the number of resource blocks K in $\mathcal{B}_u$ is an integer. This means g_{group} would be a factor of $|\mathcal{B}_u|$. In simulations, we consider cases where $g_{\text{group}} = 1, 2, 4$. Using $g_{\text{group}} = 8$ can greatly

TABLE IV

DL LINK BUDGET CALCULATION ASSUMING
1GHZ EFFECTIVE NOISE BANDWIDTH

Parameter	Value		
Distance [m]	100	200	400
BS Configuration			
Tx Power [dBm]		20	
Antenna Gain [dBm]		18.1	
Channel			
Path loss [dB]	108	114	120
Rx Power Configuration			
Rx power w/o BF [dBm]	-69.9	-75.9	-81.9
Noise Figure		12	
Noise Power		-83.9	
Shadow Fading		4.2	
Rx DL SNR [dB]	-2.2	-8.2	-14.2

enhance the rate of UEs but there will be only 4 RBs in $\mathcal{B}_u$ to avoid collisions.

- *User active rates* p: For the ease of implementation in our simulations, p exclusively controls how many active users are added per frame. Specifically, in each frame we consider 1000 new links uniformly distributed in a semi-circle covered by the rainbow beam pattern. Activations of these new UEs are treated as independent events, i.e., U as a random variable follows binomial distribution $U \sim B(1000, p)$. These new users will contend with persistent users added in a previous frame.

Given N_B, specifications of link budget at different distances are given in Table IV. The network is assumed to operate at $60\,\text{GHz}$ carrier frequency at which free space path loss model in [18] is adopted with line-of-sight (LoS) pathloss exponent equal to 2. Specifically, DL noise power is calculated based on BS's active bandwidth of $1\,\text{GHz}$, i.e., a UE's receiving signal-to-noise ratio (SNR) is independent of its active bandwidth.

With the radius of coverage, the activation rate p, and the current frame length (specified in Table III), one can compute user capacity of the system. For instance, a $400\,\text{m}$ radius of coverage and $p = 0.03$ gives the following density on average:

$$
\begin{aligned}
\rho &= \frac{\mathbb{E}[U]}{\pi \times 400^2 \times 0.5} \times \frac{1}{T_{\text{frame}}} \\
&= \frac{1000 \times 0.03}{\pi \times 400^2 \times 0.5} \times \frac{1}{125 \times 10^{-6}} \\
&\approx 0.95
\end{aligned}
\tag{14}
$$

in unit of UE activation per m^2 per second. This density ρ serves as a generic metric that evaluates network capacity.

A perceivable drawback of the proposed system is the low spectral efficiency. The drawback comes from the following facts:

- UE packets are short such that good coding schemes are not applicable. Non-payload portions cannot be ignored.
- UEs trade its bandwidth for low rate of collisions.

Even if $g_{\text{group}} = 4$ is employed along with 16-quadrature amplitude modulation (QAM) and $1/2$ coding scheme, maximum R_{eff}[10] for a single UE is merely $\frac{4 \times 18}{125 \times 10^{-6}} \times 4 \times \frac{2}{3} = 1.536$ Mbps. Thus the proposed system is not intended for high rate applications.

[10]The maximum rate is when a UE always succeeds in its first attempt of contention.
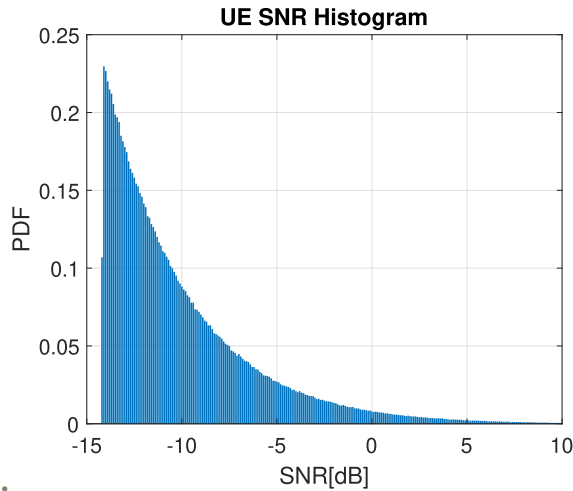
Fig. 5.   2D uniform user distribution in a semi-circle with 400m radius.

Fig. 6.   DL detection with $L = 22$ symbols, with $B = 2048$ SCs and $N_{\mathrm{B}} = 64$ antenna elements, $B/N_{\mathrm{B}} = 32$.

In the evaluation we use the following parameters unless otherwise specified. The BS has an array size of $N_{\mathrm{B}} = 64$ elements. The total number of SC is $B = 2048$ and UEs operate on $|\mathcal{B}_u| = B/N_{\mathrm{B}} = 32$ SCs. A maximum UE transmit power is set to $23\,\mathrm{dBm}$ which provides a coverage of 400m to achieve about $10\,\mathrm{dB}$ SNR for UL transmission. For users near the cell edge, due to their very low SNR, multiple synchronization attempts might be needed to ensure a satisfying detection performance. We evaluate the probability of successful synchronization as a function of SNR and its impact on access latency.

An overall histogram of DL SNR values for UEs randomly distributed in a semi-circle of $400\,\mathrm{m}$ radius is given in Figure 5. This range of SNR values are used throughout simulations.

A. Synchronization Performance

Through Monte Carlo simulations, we explore probability of correct estimation of D_u^* as a function of broadband SNR. Figure 6 gives detailed comparison of synchronization performance with and without including impacts of the afore-mentioned gain loss and a multiple-path channel. As specified in Table III, a PN sequence with length $L = 22$ is employed as preamble.

The results in Figure 6 clearly show that the gain loss has a non-negligible impact. The more SCs are used for narrowband transmission, the larger the impact of beamforming gain loss is. As $|\mathcal{B}_u|$ approaches B/N_{B}, the synchronization performance starts to saturate.

With only $|\mathcal{B}_u| = 8$ SCs in band, probability of successful synchronization is not visibly impacted by the rainbow beam pattern. This means that with $|\mathcal{B}_u| \leq B/4N_{\mathrm{B}}$, i.e., only a small number of SCs included in $\mathcal{B}_u$, the impact of rainbow beamforming is trivial. With 16 or 32 SCs in band, synchronization performance loss due to distortion becomes noticeable. There is a $4\,\mathrm{dB}$ equivalent SNR loss due to distortion when system uses $|\mathcal{B}_u| = 32$ SCs, which is effectively the threshold for $|\mathcal{B}_u|$ as discussed previously. In such case, the detection performance is merely comparable with the case of $|\mathcal{B}_u| = 16$ when there is no distortion.
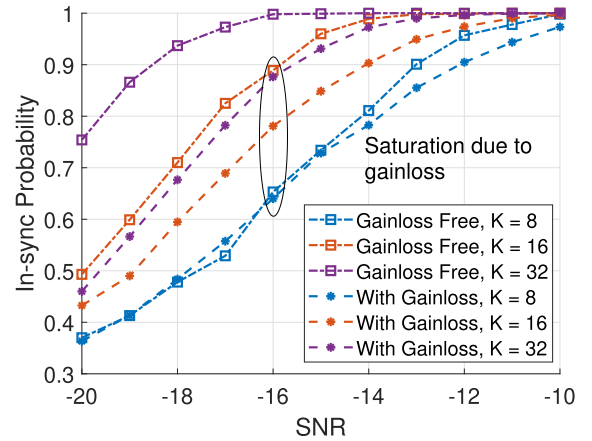
The implications of numerical results are the following. Firstly, the proposed narrowband synchronization beacon is robust to both thermal noise and frequency selectivity introduced by the rainbow beam. In a typical use case of mmW IoT with large number of devices, high probability of DL synchronization can be achieved. Secondly, synchronization performance would benefit greatly from an accurate estimation of $b_u^\star$ where (9) can then be altered to count for the gain loss coherently. Otherwise, our analysis suggests that $|\mathcal{B}_u| \leq B/4N_{\mathrm{B}}$ can be a generic threshold for achieving negligible beamforming gainloss.

B. Collision and Packet Loss Rate

Figure 7 presents both the simulated and theoretical packet loss rate given by (10). In the evaluation, we focus on the two cases $g_{\mathrm{group}} = 1, 2$.

We have the following observation from the results. Firstly, the theoretical results agree well with simulations for small and moderate n values. This confirms the correctness of the Proposition 1 where we derived PLR. Admittedly, discrepancy occurs for large n values because our derivation omitted the cases when each user uses repetition transmission that occupies the entire band. Secondly, the results indicate that for a given number of active users, there is an optimal value of repetitions that minimizes P_{PLR}. The optimal value of n decreases with an increasing number of active users in contention. This makes sense since intuitively users should avoid making too many repetitions when the network is crowded, so as to leave resources for others. Lastly, compared to probability of failed synchronizations, packet losses due to collisions among users have much smaller probabilities in the given network settings. Results from Figure 7 show that even with $g_{\mathrm{group}} = 2$ and with 20 active users transmitting simultaneously, the packet loss rate is still below 10^{-3}. With multiple retransmissions, the system can then provide high reliability.

C. Latency and Rates

Next we evaluate the total latency T_{tot} due to DL synchronization and UL contention. Here we focus on the trade-off
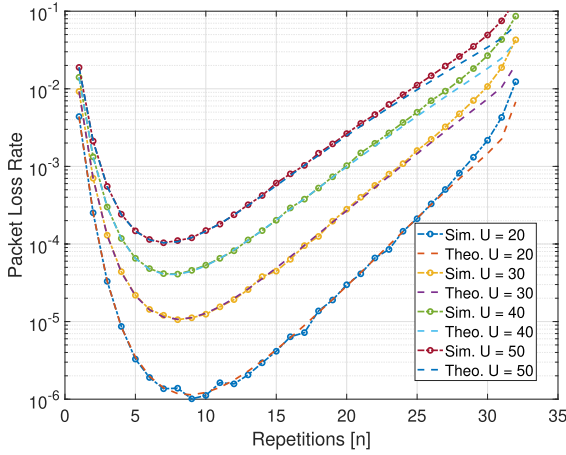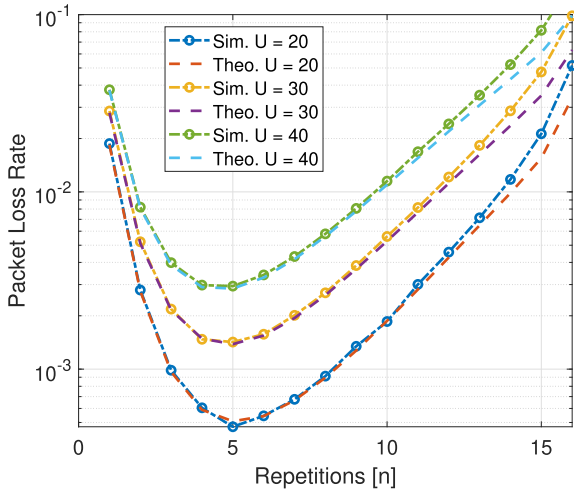
(a) Packet loss rate with UE's bandwidth as wide as $K = 32$ RBs.

(b) Packet loss rate with UE's bandwidth as wide as $K = 16$ RBs.

Fig. 7. Packet loss rate P_{PLR} as function of UE's repetition transmission number n. Different curves are evaluated with different number of active users U in contention. The optimal n drifts slowly to smaller values as U increases.
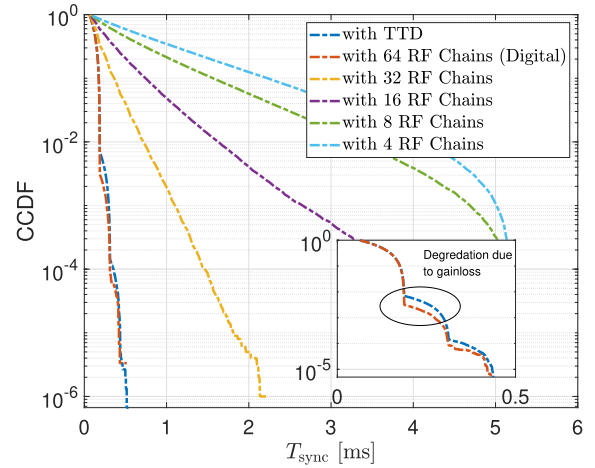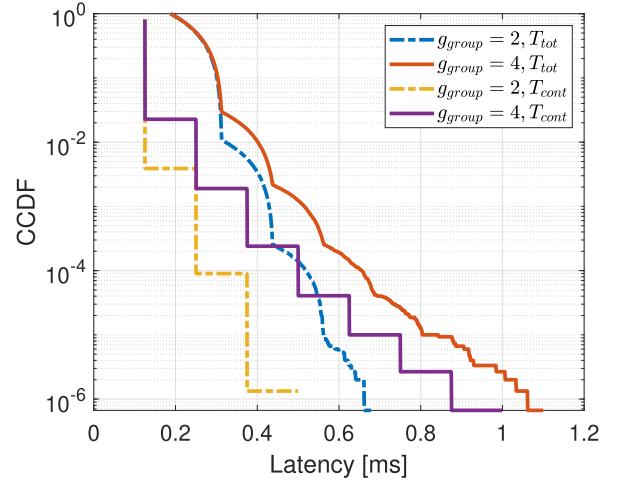

(a) Statistics for T_{sync} compared with phased array

(b) Statics for T_{tot} with different sizes of RBs.

Fig. 8. Simulated statistics of latency with active rate $p = 0.03$. T_{cont} exhibits a typical zig-zag pattern due to multiple contention attempts.

based on g_{group} as specified in IV-C. We note here again that users are generated with uniform distribution in a 2D-sector of $400\,\text{m}$ radius and activation probability of 0.03 per frame over 1000.

Simulation results for user-plane latency are presented in Figure 8. In Figure 8a, a comparison on synchronization overhead between the proposed TTD array and phased arrays with multiple RF chains is presented. In both cases, UEs operate on only 32 SCs and BS has a 64-element array. To make a fair comparison, in the case of phased array BS employs random beamforming strategy. In each frame, it steers analog beams randomly to serve users. Thus in both cases, there is no overhead due to control signaling or scheduling.[11] From the result, the performance of the proposed system approaches that of a fully-digital array. As discussed in the previous

[11]Presumably, the number of beams that a BS can steer with the phased array is limited by the number of RF chains. Since all RF chains share the same band resources, BS should point them to distinct angular sectors to cover as many users as possible. In our comparison all sectors have a equal probability to be chosen. To our best knowledge, this is the only regime with phased array that's compatible with a grant-free multiple access scheme as depicted in Figure 3.

section, the degradation comes from beamforming gainloss due to frequency dependent beam pattern. For conventional phased arrays, as the number of RF chains decrease, the overall beam coverage is limited as depicted in Figure 1. UEs start to experience prohibitively long synchronization overhead that cannot satisfy requirements of latency-critical uses cases.

The Figure 8b shows that with 2-grouping and active rate $p = 0.03$, T_{sync} dominates the overall latency while with 4-grouping, T_{cont} dominates the overall latency. The tail in contention latency is due to persistent, spatially clustered users in certain narrow band segment. Although in both cases the general URLLC requirement for reliability greater than $1 - 10^{-5}$ at $1\,\text{ms}$ latency is satisfied, in 4-grouping case the margin is small. This means that 2-grouping can still support more active users per frame (higher active probability p) while in 4-grouping case $p = 0.03$ is nearly the maximum activity rate it can support for URLLC.

In Figure 9, we show the effective rates for different grouping strategies. For instance, subcarrier grouping with $g_{\text{group}} = 4$ achieves higher rates than $g_{\text{group}} = 2$ yet users are more likely to collide. As stated before, the proposed
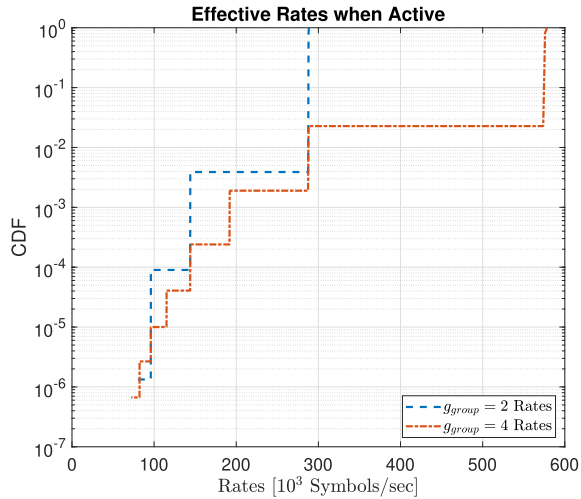
Fig. 9. Rate of a single UE with active probability $p = 0.03$ based on contention delay T_{cont} shown in Figure 8. Actual rates in bits per second depend on modulation and coding schemes.

design is tailored for URLLC and for sporadic, latency critical transmissions. Higher grouping ratio g_{group} might bring higher rates, but is very unlikely to satisfy URLLC requirement.

In Figure 10, we demonstrate trade-off of g_{group} with respect to network capacity. Specifically, we gradually increase p to see what's the approximate maximum traffic that the network can support with $g_{\text{group}} = 1$ and $g_{\text{group}} = 4$, respectively. The saturation for $g_{\text{group}} = 1$ appears at about $p = 0.165$ and as mentioned earlier the saturation for $g_{\text{group}} = 4$ appears at about $p = 0.03$. Using Equation 10, we numerically calculate P_{PLR} and find that the optimal number of repetitions n are 5 and 3, respectively. Although with $g_{\text{group}} = 1$, each user has only one forth of the data rate, BS can serve 5 times as many users as that in the case of $g_{\text{group}} = 4$.

In both cases, the achievable latency for a reliability of $1 - 10^5$ is very close to $1\,\text{ms}$, as can be seen from Figure 10. Although in the first case there is no grouping and rate of each user is small, the system can still achieve a higher sum rate on average by serving more users. With $p = 0.165$, a 16-QAM, and $1/4$ coding rate, the aggregated throughput can reach $28\,\text{Mbps}$ Mbps on BS side. In this case, the BS serves on average 165 active, low-rate users per frame. Thus the proposed system is better utilized when handling massive multiple access with stringent latency and reliability requirements.

VI. DISCUSSION AND FUTURE WORK

In this section, we briefly discuss the implications of numerical results and open research questions.

The narrow bandwidth and number of SCs used by the UE are critical parameters for system performance. With the increased number of SCs that UE can access, there is improvement in both synchronizations and contentions. On the other hand, the physical nature of rainbow beamforming limits the number of SCs (approximately B/N_{B}) that a user can access: only a fraction of radio resources are aligned with
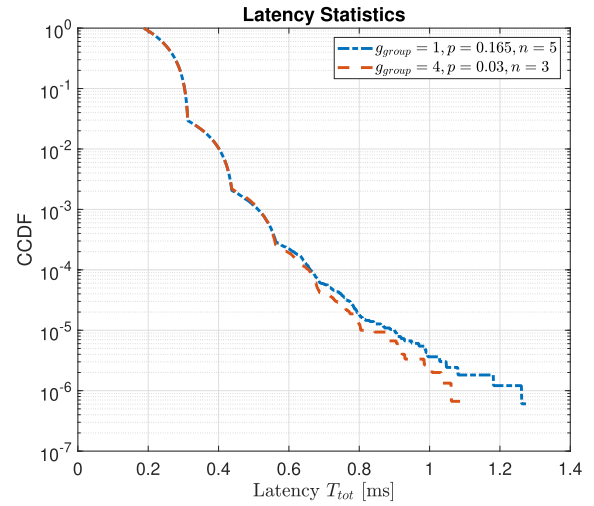
(a) Nearly Saturated Latency Statistics
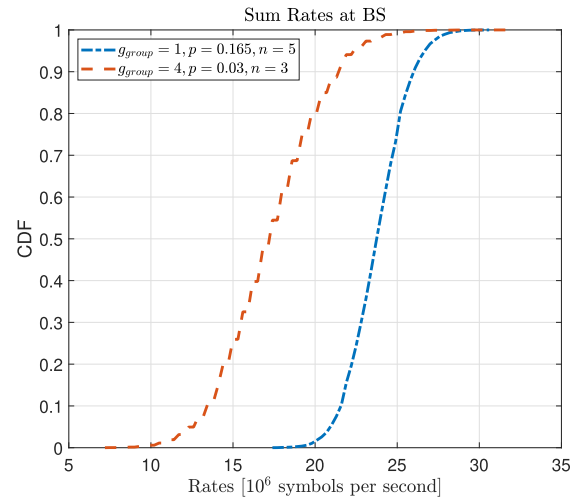
(b) Aggregated Throughput

Fig. 10. Latency and rates with different active probabilities. The $p = 0.03$ curve is the same as that in previous results.

the AoA of a UE and SCs at edge of the segment $\mathcal{B}_u$ suffer severely from beamforming mismatch.

Based on the presented analysis, the proposed system has the following performance:

- *Power and Coverage*: The proposed rainbow link based network can achieve a coverage up to $400\,\text{m}$ when BS with 64 TTD analog antenna array serves single antenna UEs with the transmit power of $23\,\text{dBm}$ assuming line-of-sight condition.
- *Rates and user capacity*: The BS can serve up to 5 active UEs per second per m^2 with Mbps data rates depending on the grouping of SCs per RB.
- *Latency and reliability*: The UEs experience $1\,\text{ms}$ latency and reliability higher than $1 - 10^{-5}$ when the optimal number of repetitions n is used.

The greatest strength of the proposed system is its flexibility to support combined URLLC and massive multiple access. Based on the proposed design of numerology and multiple access protocol, the system is better suited to serve a massive

number of users than to provide high data rates. When conservative grouping is used (in our case no grouping or 2-grouping), the proposed system can eventually achieve a sum rate at BS higher than that of the case with larger grouping.

The open research questions include but are not limited to the following:

Efficient Frame Design: If no grouping is used, one frame has only 18 symbols in its payload based on the proposed frame design. Typical URLLC packets have 32 bytes, so either dense modulation scheme or more aggressive grouping strategies would have to be used. In this work we assume $1:1$ UL DL ratio. Alternative frame design, for instance, a frame length of $250\,\mu s$ with $1:3$ UL and DL ratio could support higher data rate for each user with extra DL TTIs all contributing to the payload.

Robustness for Non-LoS channels and user mobility: In the current discussion, UEs are assumed to be in LoS channels. But the same discussion might not be applicable for non-LoS channel conditions. For instance, when a UE suffers from blockage, it loses track of its anchor SC and needs to switch to a different path. As pointed out in III-A, the switching of $\mathcal{B}_u$ without any prior requires prohibitively long overheads. Thus the current design is not robust to mobility of UEs and non-LoS channel conditions. These questions need to be addressed for practical implementations of rainbow-link.

Dynamic Control of Random Access: Increasing bandwidth of the narrowband UE, at the expense of the hardware cost, can greatly boost performance of the proposed system. While we analyzed the system performance under uniform user distribution, distributions of users based on clustered model could further intensify contentions. In this case there might be no optimal number of repetitions as the UEs would persistently contend with other UEs in the same spatial sector. To overcome this effect, the BS can control the number of repetitions that each user can make. If there are too many collisions, BS would tell each UE to reduce its repetitions so as to make sure that at least some UEs can transmit.

Alternative Multiple Access Protocol: The proposed system can benefit from non deterministic repetition coding strategy. As it has been proposed in [31], each user can use a random number of repetitions n for each contention period. This might increase system robustness to clustered scenario. Unfortunately, the analysis used in [31] is not directly applicable due to its assumption of sufficient length of code words. Alternatively, instead of repetition coding, a non-orthogonal coding can be applied. Each user can transmit data on all SCs in its band and multiply data symbols with a unique code in frequency domain. Though collisions will happen on SCs, BS can still decode with these unique code words. This is similar to [32] where NOMA is employed for multiple access.

VII. Conclusion

In this work we proposed a novel frequency domain multiple access, referred as rainbow link, that exploits wideband spectrum at mmW to serve a large number of narrowband users. By exploiting TTD array architecture at the BS, frequency resources are mapped to specific spatial directions so that users

can be assigned a subset of SCs in OFDMA and leverage beamforming gain of the entire array. Rainbow link enables a grant free multiple access and can support a very large number of users with stringent latency requirements. With a single RF chain and 64-element array, the BS can provide reliable access with $400m$ LoS coverage and sub-millisecond overhead for up to 5 UE activations per second per square meter. We believe the proposed rainbow-link can be a candidate for future critical mMTC use cases.

Appendix

A. Generic Formula for Set Covering Distribution

For the simplicity of notation, in the appendix we use B for the total number of RBs so that it integrates g_{group}. Before the detailed of derivation of (10), we first rewrite it in a more intuitive manner:

$$P_{\text{PLR}}(U, K, B, n) = \sum_{i=1}^{U-1} f\left(U-1, \frac{2K-1}{B}, i\right) \times P_{K,n}(i), \tag{15}$$

$P_{K,n}(i)$ is probability of packet loss of a user given i other users are transmitting on nearby SCs in its narrow baseband $\mathcal{B}_u$. Specifically, nearby SCs actually refer to the $(2K-1)$ SCs whose narrow band segments have intersection with $\mathcal{B}_u$. Since the user's choice of n SCs are completely random, $P_{K,n}(i)$ can be decomposed in a straight forward manner:

$$P_{K,n}(i) = \sum_{j=0}^{K} P(j \text{ among } K \text{ SCs occupied by } i \text{ users})$$
$$\times C_j^n / C_K^n \tag{16}$$

Essentially, packet loss results in the case when all n choices of the user fall on occupied SCs. Therefore, once we know the probability distribution of the number of occupied SCs, packet loss rate can be thoroughly calculated. The strategy here is to characterize occupancy of the selected narrow band as a Markov chain where each competing user causes transition of states in terms of number of occupied SCs. Let $\mathbf{p}_i \in \mathbb{R}^{K+1}$ be the vector characterizing state of the narrow band with i competing users, i.e., $[\mathbf{p}_i]_j = P(j \text{ among } K \text{ SCs occupied by } i \text{ users})$. Correspondingly, let $\mathbf{T} \in \mathbb{R}^{(K+1) \times (K+1)}$ be the transition matrix created by a single competing users. Specifically,

$$\begin{aligned}[\mathbf{T}]_{m_1, m_2} &= P(\text{new } m_2 - m_1 \text{ occupied SCs}) \\ &= \sum_{j=0}^{n} \sum_{k=1}^{K} P(\text{user occupies band with } k \text{ overlap}) \\ &\times P_k(\text{user adds } j \text{ repetitions in band}) \\ &\times P(j \text{ repetitions add } m_2 - m_1 \text{ new occupations})\end{aligned} \tag{17}$$

Since any segment of joint K SCs can be chosen as a narrow band, competing users can have different numbers of overlapping SCs with the user of interest. As a consequence, for a competing user, its n repetitions might fall only partially on

those overlapped SCs. Then, those repetitions (on overlapped SCs) contributed by a competing user may or may not land on occupied SCs in $\mathcal{B}_u$. All these probabilities are given by:

- Overlapping configurations:

$$P\left(\text{user occupies band with } k \text{ overlap}\right)$$
$$= \begin{cases} 2/(2K-1), & 1 \le k \le K-1 \\ 1/(2K-1), & k = K \end{cases}$$

- Probability that a user with a band that has K overlapped blocks with $\mathcal{B}_u$ contributes to j repetitions:

$$P_k\left(\text{user adds } j \text{ repetitions in band}\right) = \frac{\mathrm{C}_{K-k}^{n-j}\mathrm{C}_k^j}{\mathrm{C}_K^n}$$

- Probability for newly added repetitions to cause transition:

$$P\left(j \text{ repetitions add } m_2 - m_1 \text{ new occupations}\right)$$
$$= \frac{\mathrm{C}_{K-m_1}^{m_2-m_1}\mathrm{C}_{m_1}^{j-(m_2-m_1)}}{\mathrm{C}_K^j}$$

This formula is essentially a generic approximation. To our best knowledge, the exact formula here can not be tracked analytically. The main reason is that probabilities for different configurations of j repetitions in $\mathcal{B}_u$ are not even. Competing users with a highly overlapped band might generate some configurations that other users cannot. This means that state of the band can not be fully characterized by the number of occupied SCs alone.

Since a complete treatment is computationally infeasible, we here assume that all configurations for j repetitions are equivalent. This assumption works well for small and medium value of n and introduces deviation for n approaching K.

With the transition matrix, calculation of $\mathbf{p}_i$ is relatively simple:

$$\mathbf{p}_i = \mathbf{T}^i \mathbf{p}_0 \tag{18}$$

And then:

$$P_{K,n}(i) = \sum_{j=0}^{K} \left[\mathbf{T}^i \mathbf{p}_0\right]_j \mathrm{C}_j^n / \mathrm{C}_K^n \tag{19}$$

REFERENCES

[1] M. Wollschlaeger, T. Sauter, and J. Jasperneite, "The future of industrial communication: Automation networks in the era of the Internet of Things and industry 4.0," *IEEE Ind. Electron. Mag.*, vol. 11, no. 1, pp. 17–27, Mar. 2017.

[2] *NR-Lite for Industrial Sensors and Wearables*, Standard 3GPP, RP 191047, Jun. 2019. [Online]. Available: https://www.3gpp.org/ftp/TSG_RAN/TSG_RAN/TSGR_84/Docs/

[3] *NR-Lite for Rel-17 Qualcomm Views*, Standard 3GPP, RP 190844, Jun. 2019. [Online]. Available: https://www.3gpp.org/ftp/tsg_ran/TSG_RAN/TSGR_84/Docs

[4] P. Popovski, "Ultra-reliable communication in 5G wireless systems," in *Proc. 1st Int. Conf. 5G Ubiquitous Connectivity*, 2014, pp. 146–151.

[5] X. Chen, D. W. K. Ng, W. Yu, E. G. Larsson, N. Al-Dhahir, and R. Schober, "Massive access for 5G and beyond," *IEEE J. Sel. Areas Commun.*, vol. 39, no. 3, pp. 615–637, Mar. 2021.

[6] *Key Directions for Release 17*, Standard 3GPP RP 190831, Jun. 2019. [Online]. Available: https://www.3gpp.org/ftp/tsg_ran/TSG_RAN/TSGR_84/Docs

[7] J. Ding, M. Nemati, S. R. Pokhrel, O.-S. Park, J. Choi, and F. Adachi, "Enabling grant-free URLLC: An overview of principle and enhancements by massive MIMO," *IEEE Internet Things J.*, vol. 9, no. 1, pp. 384–400, Jan. 2022.

[8] N. H. Mahmood, R. Abreu, R. Bohnke, M. Schubert, G. Berardinelli, and T. H. Jacobsen, "Uplink grant-free access solutions for URLLC services in 5G new radio," in *Proc. 16th Int. Symp. Wireless Commun. Syst. (ISWCS)*, Aug. 2019, pp. 607–612.

[9] S. Dutta, M. Mezzavilla, R. Ford, M. Zhang, S. Rangan, and M. Zorzi, "Frame structure design and analysis for millimeter wave cellular systems," *IEEE Trans. Wireless Commun.*, vol. 16, no. 3, pp. 1508–1522, Mar. 2017.

[10] H. Hassanieh, O. Abari, M. Rodriguez, M. Abdelghany, D. Katabi, and P. Indyk, "Fast millimeter wave beam alignment," in *Proc. Conf. ACM Special Interest Group Data Commun.*, Aug. 2018, pp. 432–445.

[11] R. Ford, M. Zhang, M. Mezzavilla, S. Dutta, S. Rangan, and M. Zorzi, "Achieving ultra-low latency in 5G millimeter wave cellular networks," *IEEE Commun. Mag.*, vol. 55, no. 3, pp. 196–203, Mar. 2017.

[12] H. Yan, V. Boljanovic, and D. Cabric, "Wideband millimeter-wave beam training with true-time-delay array architecture," in *Proc. 53rd Asilomar Conf. Signals, Syst., Comput.*, Nov. 2019, pp. 1447–1452.

[13] E. Ghaderi, A. S. Ramani, A. A. Rahimi, D. Heo, S. Shekhar, and S. Gupta, "An integrated discrete-time delay-compensating technique for large-array beamformers," *IEEE Trans. Circuits Syst. I, Reg. Papers*, vol. 66, no. 9, pp. 3296–3306, Sep. 2019.

[14] B. Zhai, A. Tang, C. Peng, and X. Wang, "SS-OFDMA: Spatial-spread orthogonal frequency division multiple access for terahertz networks," *IEEE J. Sel. Areas Commun.*, vol. 39, no. 6, pp. 1678–1692, Jun. 2021.

[15] N. J. Karl, R. W. Mckinney, Y. Monnai, R. Mendis, and D. M. Mittleman, "Frequency-division multiplexing in the terahertz range using a leaky-wave antenna," *Nature Photon.*, vol. 9, pp. 717–720, Sep. 2015.

[16] J. Tan and L. Dai, "Delay-phase precoding for THz massive MIMO with beam split," in *Proc. IEEE Global Commun. Conf. (GLOBECOM)*, Dec. 2019, pp. 1–6.

[17] S. R. Pokhrel, J. Ding, J. Park, O.-S. Park, and J. Choi, "Towards enabling critical mMTC: A review of URLLC within mMTC," *IEEE Access*, vol. 8, pp. 131796–131813, 2020.

[18] A. Ghosh *et al.*, "Millimeter-wave enhanced local area systems: A high-data-rate approach for future wireless networks," *IEEE J. Sel. Areas Commun.*, vol. 32, no. 6, pp. 1152–1163, Jun. 2014.

[19] C.-C. Lin *et al.*, "A 4-Element 800MHz-BW 29 mW true-time-delay spatial signal processor enabling fast beam-training with data communications," in *Proc. IEEE 47th Eur. Solid State Circuits Conf. (ESSCIRC)*, Sep. 2021, pp. 287–290.

[20] C.-D. Chung and W.-C. Chen, "Preamble sequence design for spectral compactness and initial synchronization in OFDM," *IEEE Trans. Veh. Technol.*, vol. 67, no. 2, pp. 1428–1443, Feb. 2018.

[21] B. Singh, O. Tirkkonen, Z. Li, and M. A. Uusitalo, "Contention-based access for ultra-reliable low latency uplink transmissions," *IEEE Wireless Commun. Lett.*, vol. 7, no. 2, pp. 182–185, Apr. 2018.

[22] T. Jacobsen *et al.*, "System level analysis of uplink grant-free transmission for URLLC," in *Proc. IEEE Globecom Workshops (GC Wkshps)*, Dec. 2017, pp. 1–6.

[23] Y. Liu, Y. Deng, M. Elkashlan, A. Nallanathan, and G. K. Karagiannidis, "Analyzing grant-free access for URLLC service," *IEEE J. Sel. Areas Commun.*, vol. 39, no. 3, pp. 741–755, Mar. 2021.

[24] Y.-P. E. Wang *et al.*, "A primer on 3GPP narrowband Internet of Things," *IEEE Commun. Mag.*, vol. 55, no. 3, pp. 117–123, Mar. 2017.

[25] T. Levanen, J. Pirskanen, and M. Valkama, "Radio interface design for ultra-low latency millimeter-wave communications in 5G era," in *Proc. IEEE Globecom Workshops (GC Wkshps)*, Dec. 2014, pp. 1420–1426.

[26] H. Ji, S. Park, J. Yeo, Y. Kim, J. Lee, and B. Shim, "Ultra-reliable and low-latency communications in 5G downlink: Physical layer aspects," *IEEE Wireless Commun.*, vol. 25, no. 3, pp. 124–130, Jun. 2018.

[27] G. Durisi, T. Koch, and P. Popovski, "Toward massive, ultrareliable, and low-latency wireless communication with short packets," *Proc. IEEE*, vol. 104, no. 9, pp. 1711–1726, Aug. 2016.

[28] A. A. Zaidi, R. Baldemair, V. Moles-Cases, N. He, K. Werner, and A. Cedergren, "OFDM numerology design for 5G new radio to support IoT, eMBB, and MBSFN," *IEEE Commun. Standards Mag.*, vol. 2, no. 2, pp. 78–83, Jun. 2018.

[29] R. Mullner, C. F. Ball, K. Ivanov, J. Lienhart, and P. Hric, "Contrasting open-loop and closed-loop power control performance in UTRAN LTE uplink by UE trace analysis," in *Proc. IEEE Int. Conf. Commun.*, Jun. 2009, pp. 1–6.

[30] X. Lin, A. Adhikary, and Y.-P. E. Wang, "Random access preamble design and detection for 3GPP narrowband IoT systems," *IEEE Wireless Commun. Lett.*, vol. 5, no. 6, pp. 640–643, Dec. 2016.

[31] G. Liva, "Graph-based analysis and optimization of contention resolution diversity slotted ALOHA," *IEEE Trans. Commun.*, vol. 59, no. 2, pp. 477–487, Feb. 2011.

[32] Z. Ding, P. Fan, and H. V. Poor, "Random beamforming in millimeter-wave NOMA networks," *IEEE Access*, vol. 5, pp. 7667–7681, 2017.

Han Yan (Member, IEEE) received the B.E. degree from Zhejiang University, Hangzhou, China, in 2013, and the M.S. and Ph.D. degrees in electrical and computer engineering from UCLA in 2015 and 2020, respectively. He has broad research interests in signal processing and communication system design for millimeter-wave mobile networks, cooperative unmanned aerial vehicles networks, and dynamic spectrum sharing radios. He was a recipient of the UCLA Dissertation Year Fellowship in 2018, the Qualcomm Innovation Fellowship in 2019, the UCLA ECE Distinguished Ph.D. Dissertation Award in 2020, and the Best Paper Award at the 2020 ACM mmNets Workshop.

Danijela Cabric (Fellow, IEEE) received the M.S. degree in electrical engineering from the University of California at Los Angeles (UCLA) in 2001 and the Ph.D. degree in electrical engineering from UC Berkeley in 2007. She is currently a Professor in electrical and computer engineering with UCLA. Her research interests are millimeter-wave communications, distributed communications and sensing for the Internet of Things, and machine learning for wireless networks co-existence and security. She received the Samueli Fellowship in 2008, the Okawa Foundation Research Grant in 2009, the Hellman Fellowship in 2012, the National Science Foundation Faculty Early Career Development (CAREER) Award in 2012, and the Qualcomm Faculty Award in 2020 and 2021. She served as an Associate Editor for IEEE Transactions on Cognitive Communications and Networking, IEEE Transactions on Wireless Communications, IEEE Transactions on Mobile Computing, and *IEEE Signal Processing Magazine*. She served as an IEEE ComSoc Distinguished Lecturer.

Ruifu Li (Student Member, IEEE) received the B.Sc. degree from the University of Wisconsin–Madison in 2020. He is currently pursuing the M.S. degree in electrical and computer engineering with the University of California at Los Angeles. His research interests include signal processing and wireless communications.